Geotechnical and Geological Engineering (2006) 24: 1039–1063
DOI 10.1007/s10706-005-4431-5

Technical Note

Deformability characteristics of a rock mass under true-triaxial stress compression

RAJENDRA P. TIWARI[1] and K.S. RAO[2,*]
[1]*Department of Civil Engineering, Rewa Engineering College, Rewa 486002, MP, India*
[2]*Department of Civil Engineering, Indian Institute of Technology, New Delhi 110016, India*

(Received 24 August 2004; revised 7 March 2005; accepted 18 March 2005)

Abstract. In this paper an experimental study was planned on rock mass model with three joint sets under triaxial and true-triaxial stress states to assess the influence of joint geometry and stress ratios on deformational behaviour of rock mass. The physical models were composed of three continuous orthogonal joint sets in which joint set-I was inclined at angle $\theta = 0°$, 20°, 40°, 60°, 80° and 90° with x-axis, joint set-II was produced at staggering $s = 0.5$ and joint set-III was kept always vertical. Thus, rock mass models with medium interlocked smooth joints ($\phi_j = 36.8°$) were simulated under true triaxial compression ($\sigma_1 > \sigma_2 > \sigma_3$). Modulus of rock mass shows anisotropy with joint inclination θ which diminishes with increase in σ_2/σ_3 ratio. The rock mass at $\theta = 60°$ shows the highest modulus enhancement (599.9%) whereas it is minimum (32.3%) at $\theta = 90°$. Further two empirical expressions for estimation of deformation modulus were suggested based on experimental results, which were developed by incorporating two basic concepts, e.g. Janbu's coefficients and joint factor, J_f.

Key words. deformability, intermediate principal stress, physical modelling, rock mass, true triaxial.

1. Introduction

The deformation behaviour of a jointed rock mass is mainly influenced by the deformation of joints. Experiences show that the deformation modulus of rock masses decreases remarkably in comparison with that of intact rock when joints are present (Heuze, 1980; Li, 2001; Singh et al., 2002). The knowledge of deformation characteristics of rock mass is always an essential input in the analysis and design of any surface and subsurface civil/mining engineering projects.

The different methods for determining deformation of rock mass are field and laboratory tests and constitutive equations. The field tests, though accurate, are difficult to execute due to cost, time and accessibility reasons. In constitutive modelling, Goodman (1989) suggested expression of modulus of elasticity for rock mass by substituting it with an equivalent continuous material representing the rock mass. He assumed that the rock mass is regularly crossed by a single set of joints and the

*Corresponding author: K.S. Rao, Department of Civil Engineering, Indian Institute of Technology, Delhi, Haus Khas, New Delhi, India. e-mail: raoks@civil.iitd.ernet.in

intact rock is isotropic and linearly elastic. Huang et al. (1995) suggested expression for a rock mass with three intersecting set of joints under unconfined compression state. Li (2001) has given modified equations for jointed rock mass considering the anisotropic conditions and proposed a method for graphically presenting the modulus in upper hemisphere. The constitutive models discussed above have their limitations, as they only can be applicable in the ideal conditions of materials and stress states. The conditions at site are always complex and restrict the use of theoretical models and in such situations empirical models are always practical to use with fair accuracy. Thus, physical modelling is better option to describe the deformation characteristics of rock mass in general.

Based on field experiences, Bieniawski (1978) suggested correlation between *in situ* modulus of rock masses and rock mass rating (RMR). Similarly based on extensive experimental results on jointed rocks Ramamurthy (1993), Ramamurthy and Arora (1994) presented the ratio of moduli (ratio of modulus of jointed to the modulus of intact specimens) in unconfined state as a function of joint factor (J_f). The joint factor is defined as weakness coefficient and is composed of three important parameters: joint frequency, joint orientation and shear strength along joint and can be represented by following equation.

$$J_f = \frac{J_n}{n \cdot r} \tag{1}$$

where J_n is joint frequency or number of joint per meter length in the direction of loading, n is joint inclination parameter and r is joint shear strength parameter. He presented values between n and β (inclination of joint with vertical loading direction) and found that the variation of n with β is independent of rock type (Table 1). Ramamurthy (1993) recognized third most important parameter affecting the engineering response of jointed rock as the shear strength along sliding joint. This can be estimated by conducting a direct shear test on joint under very low normal stress. The suggested expression for estimation of joint shear strength parameter, r is as below.

Table 1. Value of inclination parameter, n for different orientations of the joint (after Ramamurthy, 1993)

Joint orientation, β° ($=90^\circ-\theta^\circ$)	Inclination parameter, n
0	0.810
10	0.460
20	0.150
30	0.046
40	0.071
50	0.306
60	0.465
70	0.634
80	0.814
90	1.000

$$r = \tan \phi_j = \frac{\tau_j}{\sigma_{nj}} \tag{2}$$

where τ_j is the shear strength along the joint, and σ_{nj} the normal stress on the joint. He also correlated the joint shear strength parameter of intact (unfilled, fresh and not weathered) joints with the uniaxial compressive strength σ_{ci} of intact rock material (Table 2). He further suggested the shear strength parameter 'r' for gouge filled joint assuming gouge soil to be in the dense state at near residual condition as given Table 3. Based on extensive experimental data on jointed rocks (Ramamurthy, 1993), the modulus in unconfined state was related to the modulus in the confined state by the following expression:

$$\frac{E_j(\sigma_3 = 0)}{E_j(\sigma_3)} = 1 - \exp\left(\frac{-0.1\sigma_{cj}}{\sigma_3}\right) \tag{3}$$

where σ_3 is the confining stress, σ_{cj} the uniaxial compressive strength of jointed rock, E_j ($\sigma_3 = 0$) and $E_j(_{\sigma 3})$ are deformation modulus of jointed rock in unconfined and confined stress states respectively.

The specimens used to conduct above studies by Ramamurthy (1993), Ramamurthy and Arora (1994) were small size cylindrical specimens of diameter 38 mm having L/D ratio 2 and always have limitations while simulating with large rock mass area at site. The large size specimens with three joint sets were used by Singh

Table 2. Suggested values of joint strength parameter, r for different values of σ_{ci} (Ramamurthy, 1993)

UCS of intact rock, σ_{ci} (MPa)	Joint strength parameter, r	Remarks
2.5	0.30	Fine grained
5.0	0.45	micaceous
15.0	0.60	
25.0	0.07	to
45.0	0.80	
65.0	0.90	Coarse
100.0	1.00	grained

Table 3. Joint strength parameter for filled joints (Ramamurthy, 1993)

Gouge description	Friction angle in degree	Joint strength parameter $r = \tan \phi_j$
Gravely sand	45	1.00
Coarse sand	40	0.84
Fine sand	35	0.70
Silty sand	32	0.62
Clayey sand	30	0.58
Clay silt		
Clay – 25%	25	0.47
Clay – 50%	15	0.27
Clay – 75%	10	0.18

et al. (2002) to eliminate the scale effect phenomenon. They conducted uniaxial compression testing on block mass specimens and linked the deformation modulus with joint factor in unconfined compression state. There was still need to conduct triaxial and true-triaxial compression testing on large size rock mass specimens to take into account different joint geometries and stress conditions, i.e. $\sigma_2 > \sigma_3$.

In present study an experimental study was planned on specimens of rock mass with three joint sets with varying joint geometry under uniaxial, triaxial and true-triaxial stress state. The results obtained were analysed to predict deformational behaviour of rock mass and also used to suggest expression for modulus in triaxial stress condition. The experimental data obtained through extensive testing have also been used to develop empirical expressions of deformation modulus in terms of Janbu's (1963) coefficients. The modulus values obtained from the two empirical methods were compared with the experimental values. The experimental results available in true-triaxial testing, were also used further to suggest expression of deformation modulus in $\sigma_2 > \sigma_3$ condition.

2. Experimentation on physical models

The physical model testing on jointed rock mass was conducted under uniaxial, triaxial and true-triaxial stress states. The true-triaxial system (TTS) developed by Rao and Tiwari (2002) was used in the present study (Figure 2a and b). Total 54 specimens were tested. The model material was chosen as sand-lime bricks with average uniaxial compressive strength 13.5 MPa and represented as 'EM' on Deere-Miller's classification chart. Its suitability to use as brittle model material was verified (Tiwari and Rao, 2003). The model material properties have been listed in Table 4.

The specimens were prepared by cutting model material bricks into small cubes of size 2.5 cm and arranging the small cubes to form the test specimen of size

Table 4. Model material properties of sand-lime blocks (after Tiwari and Rao, 2004)

Property	Range	Average value
Dry density, γ_d (kN/m^3)	16.1–17.8	16.86
Specific gravity	2.66–2.67	2.66
Absolute porosity, n (%)	32.7–39.3	36.5
UCS (intact cyl.), σ_{ci} (MPa)	11.1–15.9	13.5
Tensile strength, σ_{tb} (MPa)	1.63–2.17	1.89
Failure strain, UCS (%)	0.43–0.63	0.53
Poisson's ratio, ν	0.18–0.0.27	0.25
Tangent modulus, E_{t50} (MPa)	4782–4866	4866
Internal friction angle ($\phi°$)	–	44.7
Cohesion, c (MPa)	–	3.29
Joint friction angle ($\phi°_j$)	–	36.8
Deere–Miller's chart	–	EM

15 cm × 15 cm × 15 cm having three sets orthogonal joints. The joint set-I was continuous and inclined at various angles $\theta = 0°$, 20°, 40°, 60°, 80° and 90° with x-axis. The joint set-II was perpendicular to set-I and was kept at stepping (s) = 0.5 of width of small block. The set-III was always vertical (Figure 1). Each specimens were given unique identification number, i.e. A60/0.31/1.62 which indicates Type-A sample of $\theta = 60°$ and is acted by horizontal stresses, $\sigma_3 = 0.31$ and $\sigma_2 = 1.62$ MPa.

2.1. TESTING OF SPECIMENS

The TTS consists of a 1000 kN capacity vertical frame, a biaxial frame of 300 kN capacity fitted with two pairs of hydraulic jacks and platens, constant confining pressure unit for applying, monitoring and maintaining horizontal stresses (σ_2 and σ_3) on specimen faces, eight channel data acquisition system and personal computer to record all load and deformation data. Before testing, the prepared specimens were firstly oven dried then kept for air-drying at room temperature for 30 days. The cured specimen was carefully transferred on the vertical loading platens of true-triaxial system and all platens were moved slowly to contact the specimen faces. The friction free and uniform stress on all six faces was ensured by firstly putting 0.5 mm thick pair of Teflon sheets smeared with high vacuum silicon grease between specimen and platen and secondly by movement of horizontal frame in vertical and horizontal planes using screw levers. The final micro-adjustment of platens on specimen lateral faces was done by moving platens in vertical and horizontal plane

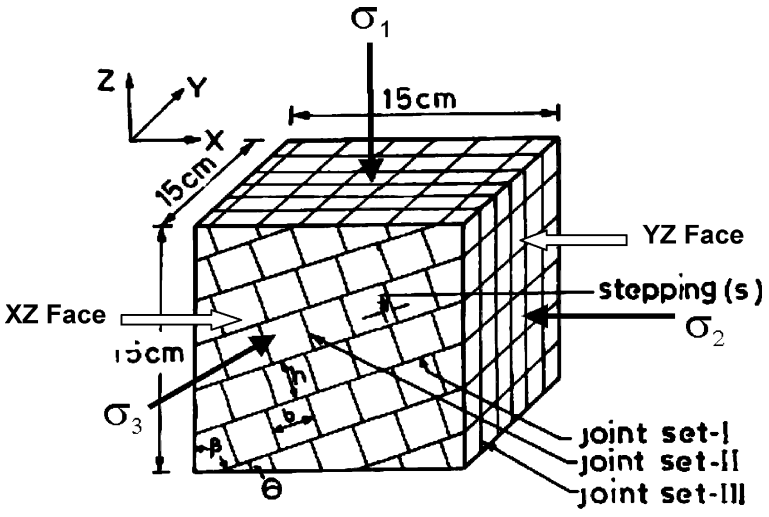

Figure 1. Key sketch of model tested (after Tiwari and Rao, 2004).

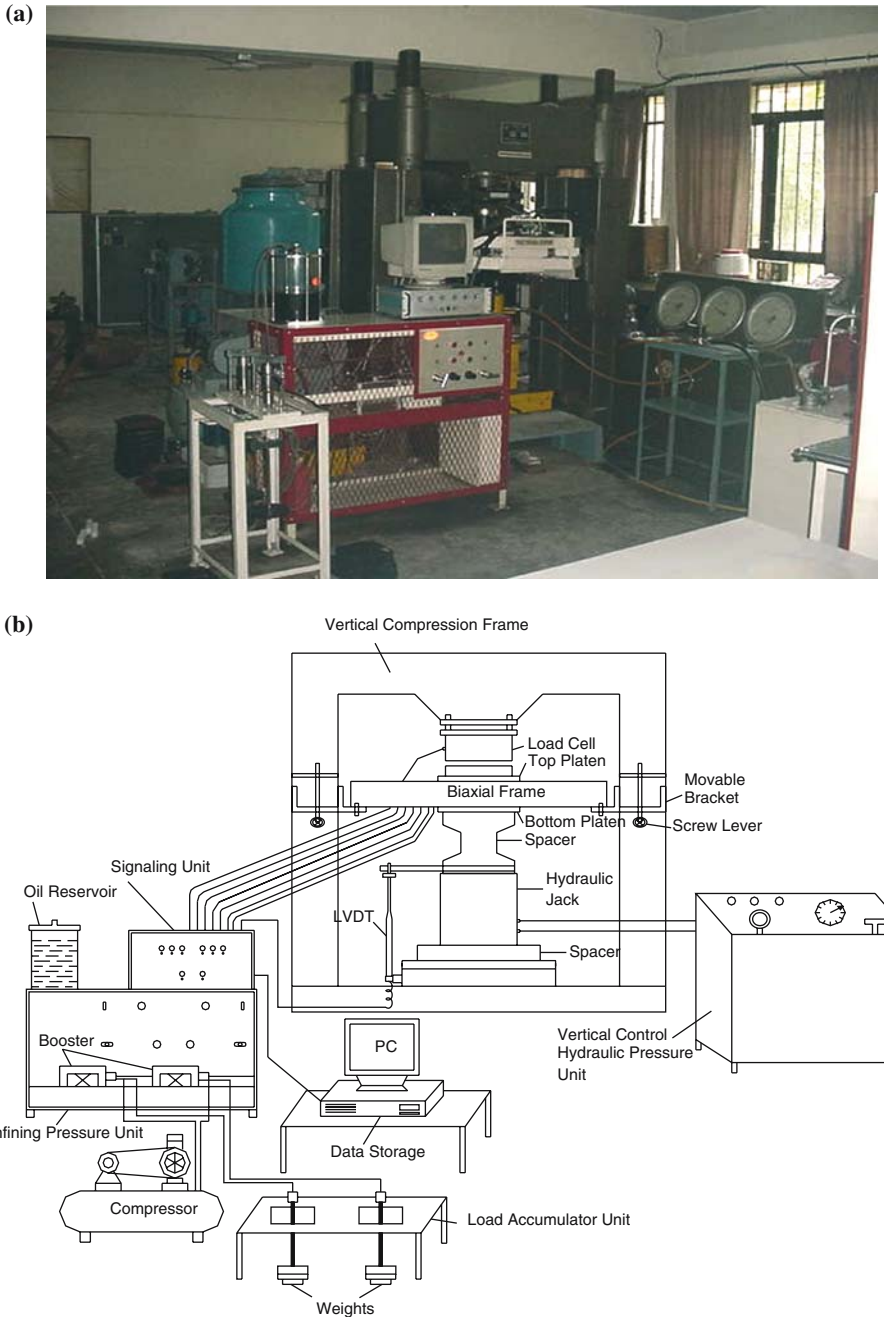

Figure 2. (a) Complete set-up of true-triaxial system (after Rao and Tiwari, 2002). (b) Schematic diagram for set-up of true-triaxial system.

with the help of screw levers fitted on biaxial frame. Now, three independent stresses were applied initially in quasi-isotropic conditions (i.e. $\sigma_1 > \sigma_2 = \sigma_3$). After reaching the pre-determined level of σ_2 and σ_3, the σ_1 was increased monotonically from $\sigma_1 = \sigma_2$ to a level when specimen yields and even in post-failure zone till residual strength of specimen (see Figure 3). The vertical deformation of specimen was recorded through LVDT attached at vertical hydraulic jack and its tip touching the base of lower loading platen. The horizontal deformation of specimen along σ_3 directions was measured through LVDT's fitted at pair of hydraulic jacks on either side of specimen faces. The sum of deformations of both LVDT's was taken as average deformation of specimen in σ_3 directions. Similarly LVDT's fitted in σ_2 directions were also used to measure the lateral deformation along σ_2 axis. The vertical loading was recorded using vertical load cell fitted on top of specimen. The lateral loads to apply σ_2 and σ_3 on lateral specimen faces were measured through two load sensors fitted in hydraulic line of horizontal jacks. The signal from five LVDT's and three load cells/sensors were continuously transferred to data acquisition system, which finally transfers them to PC as note pad data. Strain controlled vertical loading was applied at a rate of 0.75×10^{-3} cm/s in all the testing cases. Details of testing programme are listed in Table 5.

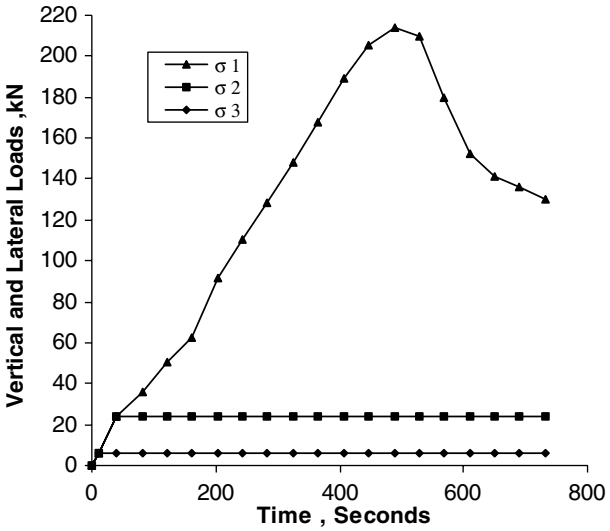

Figure 3. Typical load vs. time plot for complete testing of sample A0/0.31/1.22.

Table 5. Details of testing programme

Test cases	θ° and *s* details	σ_3 (MPa)	σ_2 (MPa)	σ_2 σ_3 axis
Type-A (54)	$s = 0.5$; θ = 0, 20, 40, 60, 80, 90	0.31	0.31, 0.59, 0.95, 1.22, 1.62	σ_2–X; σ_3–Y
		0.78	0.78, 1.22, 2.24	
		1.22	1.22	

3. Experimental findings

The recorded note pad data of load and deformation was used for analysis and area correction was made in each specimen for calculating major principal stress σ_1. The typical stress–strain curves have been plotted from the results of rock mass testing and curves show the deviotric stress ($\sigma_1-\sigma_3$) plot against axial strain (ε_1), lateral strain along σ_2 (ε_2), lateral strain along σ_3 (ε_3), and volumetric strain (ε_{ϖ}). The compressive stress and strain are considered positive whereas two tensile lateral strains are negative in general. Engineering properties such as strength, deformation modulus, modulus ratio and failure strain for each specimen are estimated using these plots.

3.1. STRESS–STRAIN CURVES

Figure 4 shows brittle failure for samples of rock mass (Type-A case) with $\theta = 0°$, 20°, 80° and 90° showing steep elastic portion up to almost the peak and gradual fall in stress (strain softening) after failure. The slope of curve increases in both regions with increase in σ_2/σ_3 ratio. Similarly, Figure 5 shows the ductile behaviour for $\theta = 40°$, 60° cases showing short elastic range followed by a continuous increase in stress and decrease in tangent modulus with increasing strain up to failure. After peak, stress increase is continued (strain hardening) in most specimens whereas stress remains constant (elastic–plastic) in few specimens depending upon joint configurations and confinement levels.

3.2. FAILURE MECHANISM

The specimens showed different failure patterns, depending upon joint configuration, stress ratio, and stress orientations. Figure 6a shows the shearing of intact material and joints which was observed in case of Type-A specimens with $\theta = 0°$, 20°, 80° and

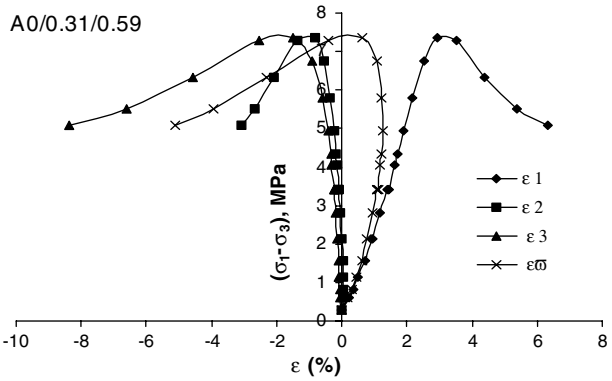

Figure 4. Stress–strain curves for rock mass specimens A0/0.31/0.59 showing strain softening behaviour.

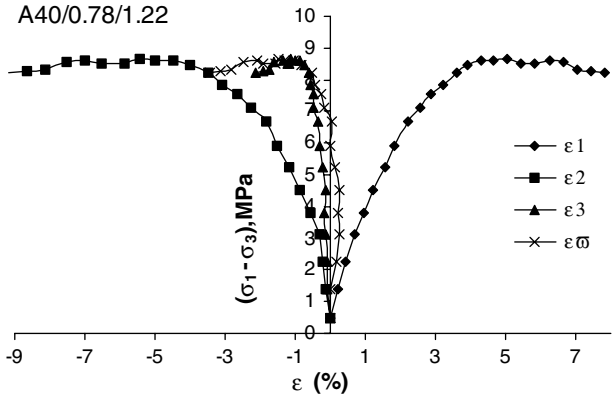

Figure 5. Stress–strain curves for rock mass specimens A40/0.78/1.22 showing elastic–plastic and strain hardening behaviour.

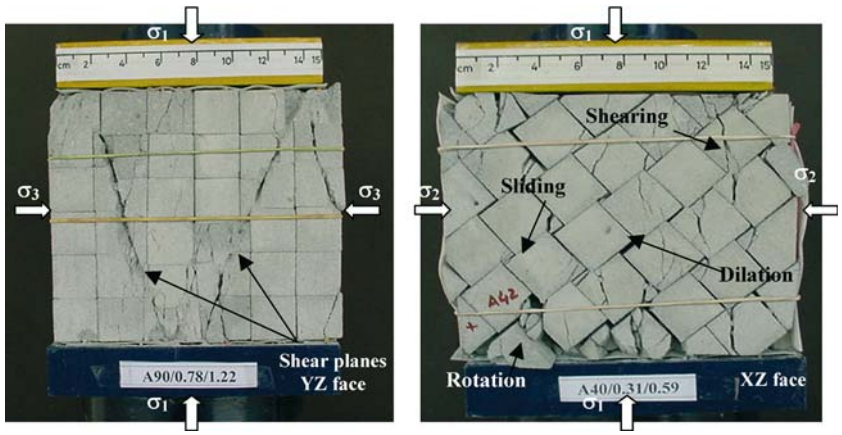

Figure 6. Failure mechanism in rock mass specimen: (a) shearing of intact blocks and joints along with shear planes on YZ face at $\theta = 90°$, (b) joint dilatation, sliding along joint plane, rotation of blocks and shearing of intact material on XZ face at $\theta = 40°$.

90°. The shear planes developed on YZ or σ_2 face dips along σ_3 direction and the fracture dip increases with increasing σ_2. Similarly, Figure 6b shows the joint dilation and shearing of some blocks (in Type-A, $\theta = 40°$) and sliding along joint mixed with shearing (in $\theta = 60°$) on XZ face. Mode of failure shifted from sliding, dilation to shearing with increasing σ_2/σ_3 ratio.

3.3. DEFORMATION MODULUS

The deformation modulus, E_{tj} is estimated as slope of tangent at point on stress–strain curve corresponding to 50% of failure stress. Figure 7a and Table 6 show that modulus values (in MPa) increase from 380.5 to 743.5 in A0, 200.0 to 569.7 in A20, 84.5 to 247.3 in A40, 32.9 to 210.4 in A60, 357.9 to 778.9 in A80 and 631.5 to 835.3 in

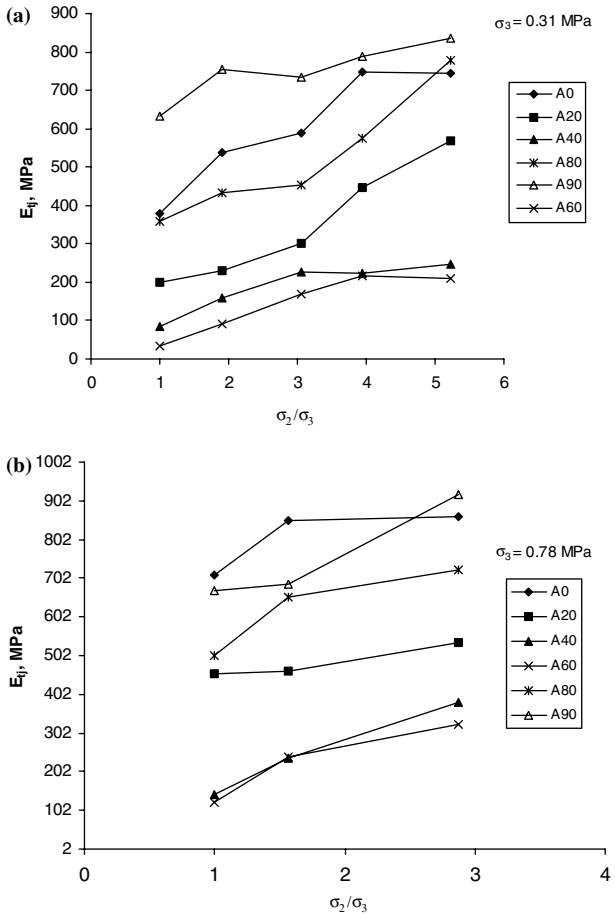

Figure 7. Effect of intermediate principal stress on deformation modulus of rock mass at σ_3: (a) 0.31 MPa, (b) 0.78 MPa.

Table 6. Deformation modulus $E_{tj(50\%)}$ values for rock mass specimens

		$E_{tj(50\%)}$ (MPa)					
		Inclination, θ (°)					
σ_3 (MPa)	σ_2 (MPa)	0	20	40	60	80	90
0.31	0.31	380.5	200.0	84.5	32.9	357.9	631.5
0.31	0.59	537.9	229.6	160.0	90.6	434.7	755.6
0.31	0.95	587.1	300.7	228.1	168.0	452.1	733.3
0.31	1.22	747.4	445.4	222.6	217.1	574.2	788.8
0.31	1.62	743.5	569.7	247.3	210.4	778.9	835.3
0.78	0.78	711.5	456.4	142.2	124.3	503.2	671.4
0.78	1.22	850.0	463.1	236.1	238.9	654.5	687.5
0.78	2.24	860.7	534.7	380.4	325.0	723.8	916.7
1.22	1.22	718.0	464.1	298.0	189.6	517.7	723.8

A90 specimens with increase of σ_2/σ_3 ratio from 1 to 5.2. The rate of increase in modulus is higher initially, which declines gradually with increasing σ_2/σ_3. The modulus is the minimum at $\theta = 60°$ and the maximum at 90°. In contrast to failure strength case, the modulus values are highly influenced by joint inclination at higher σ_2/σ_3 ratio too. Further, similar variation is observed at $\sigma_3 = 0.78$ MPa case as shown in Figure 7b and Table 6.

The initial modulus is estimated from stress–strain curves by drawing tangent at initial point of curve. The slope of this tangent line is termed as initial modulus, E_{ij} which increases with increase in σ_2/σ_3. The initial modulus, E_{ij} is observed lower than tangent modulus, E_{tj} at all joint inclination as shown in Table 7. Janbu (1963) has suggested an equation for prediction of modulus at any confining pressure for soil and intact rock. Janbu's (1963) coefficients K and n are also estimated for rock mass specimens tested in triaxial compression. The K and n parameters will be used for formulation of expressions for deformation modulus.

3.4. ANISOTROPIC BEHAVIOUR

The failure strength, deformation modulus and modulus ratio of rock mass are significantly influenced by joint configuration or inclination, θ of critical joint set-I. The variation of engineering parameters with β ($= 90° - \theta$) is known as anisotropy. The anisotropy ratio R_c is defined by the following equation:

$$R_c = \frac{\sigma_{190}}{\sigma_{1\,min}} = \frac{E_{tj90}}{E_{tj\,min}} \tag{4}$$

where σ_{190} and E_{tj90} are triaxial compressive strength and modulus values corresponding to $\beta = 90°$. The σ_{1min} and E_{tjmin} are the minimum values of these parameters near $\beta = 30°$–$50°$. The anisotropy in engineering parameters of rock mass

Table 7. Initial modulus E_{ij} values for rock mass specimens

		E_{ij} (MPa)					
		Inclination, θ (4°)					
σ_3 (MPa)	σ_2 (MPa)	0	20	40	60	80	90
0.31	0.31	190.0	141.1	119.2	68.5	148.5	312.5
0.31	0.59	200	150.2	160	115.3	391.8	426.1
0.31	0.95	394.4	162.2	273.1	197.7	739.4	434.7
0.31	1.22	538.8	172.9	312.7	362.5	825.9	558.3
0.31	1.62	937.5	486.9	488.8	475.0	972.2	787.5
0.78	0.78	455.0	362.2	245.1	230.0	417.9	655.5
0.78	1.22	1162.5	455.2	452.4	435.0	545.5	661.5
0.78	2.24	1126.8	490.0	856.5	690.0	687.5	1511.7
1.22	1.22	445.0	386.4	554.1	275.0	535.8	751.8

can be classified using Table 8. The anisotropy ratio R_c for engineering parameters reduces with increase in σ_2/σ_3 value. Deformation modulus of rock mass varies systematically with inclination of critical joint set-I. The values are maximum at $\beta = 90°$ and minimum between $\beta = 30°$ and 40° as shown in Figure 8a. Such

Table 8. Classification of anisotropy (after Ramamurthy, 1993)

R_c Range	Description	Symbol
1.0–1.1	Isotropic	I
> 1.1–2.0	Low	L
> 2.0–4.0	Medium	M
> 4.0–6.0	High	H
> 6.0	Very high	VH

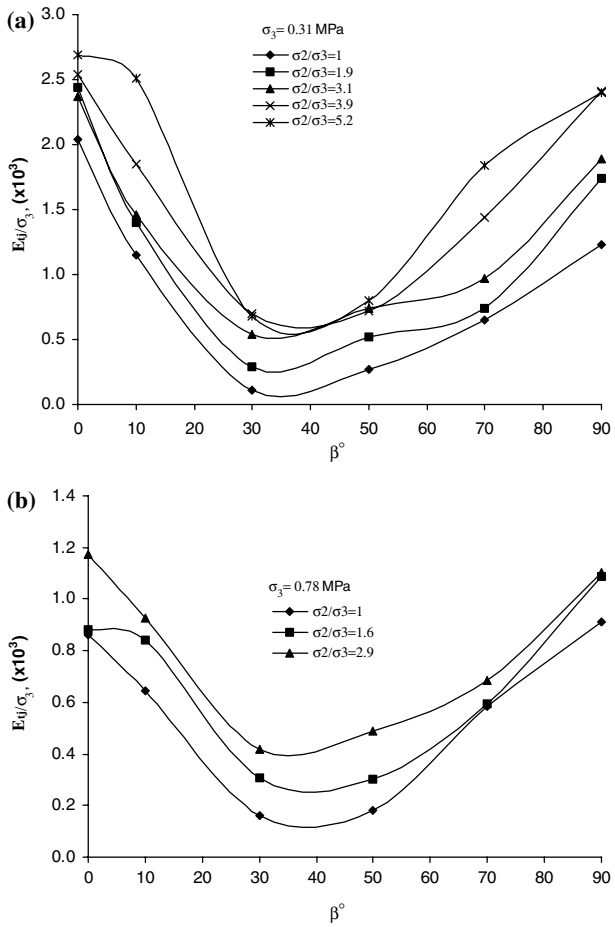

Figure 8. Modulus anisotropy in rock mass under true-triaxial compression at (a) $\sigma_3 = 0.31$ MPa and (b) $\sigma_3 = 0.78$ MPa.

anisotropy is very high (19.2) at $\sigma_2/\sigma_3 = 1$ and diminishes to medium (3.6) at higher σ_2/σ_3 ratio of 5.2 and $\sigma_3 = 0.31$ MPa. Similarly anisotropy in modulus reduces from 5.4 to 2.8 at $\sigma_3 = 0.78$ MPa (see Figure 8b and Table 9). In triaxial stress state anisotropy reduces (from 19.2 to 3.8) with increase of $\sigma_2 = \sigma_3 = 0.31$–1.22 MPa, which can be seen in Figure 9.

3.5. ENHANCEMENT IN ENGINEERING RESPONSE

The main objective of true-triaxial study was to assess the enhancement in values of engineering parameters, i.e. triaxial compressive strength and modulus values over

Table 9. Anisotropy ratio R_c in rock mass specimens

		Anisotropy ratio, R_c value					
		Strength, σ_1		Modulus, $E_{tj50\%}$		Modulus ratio, M_{rj}	
σ_3 (MPa)	σ_2/σ_3	Value	Symbol	Value	Symbol	Value	Symbol
0.31	1.0	4.0	H	19.2	VH	4.8	H
0.31	1.9	2.8	M	8.3	VH	2.9	M
0.31	3.1	2.3	M	4.4	H	2.8	M
0.31	3.9	2.0	L	3.6	M	2.4	M
0.31	5.2	1.2	L	3.9	M	3.3	M
0.78	1.0	2.7	M	5.4	H	3.1	M
0.78	1.6	2.1	M	2.9	M	2.6	M
0.78	2.9	1.6	L	2.8	M	2.4	M
1.22	1.0	2.7	M	3.8	M	1.0	L

VH: very high, H: high, M: medium, L: low.

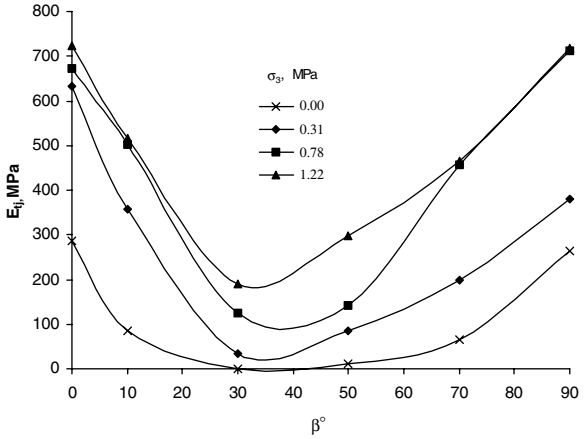

Figure 9. Modulus anisotropy in rock mass under triaxial compression.

the same obtained from conventional triaxial testing on rock mass. The triaxial compressive strength enhancement may be defined as $(\sigma_{1ttr}-\sigma_{1tr}) / \sigma_{1tr}$, where σ_{1ttr} and σ_{1tr} are true-triaxial and triaxial compressive strength respectively. Similarly modulus enhancement will be equal to as $(E_{ttr} - E_{tr})/E_{tr}$, where E_{ttr} and E_{tr} are deformation modulus in true-triaxial and triaxial stress state respectively.

The triaxial compressive strength at failure in triaxial compression further increases, when σ_2/σ_3 is increased keeping $\sigma_3 = 0.31$ MPa of constant value. This percentage increase over triaxial compressive strength is termed as strength enhancement. Table 10 show that enhancement in rock mass is equal to 36.9%, 105.2%, 192.5%, 309.2%, 73.9% and 26.1% at $\theta = 0°$, 20°, 40°, 60°, 80° and 90°, respectively. This enhancement is highest (309.2%) at $\theta = 60°$ and minimum (26.1%) at $\theta = 90°$. Thus rock mass with high uniaxial compressive strength are subjected to low strength enhancement than weak rock mass when they subjected to increase in intermediate principal stress σ_2. Haimson and Chang (2000) has also observed maximum 20% of enhancement in strength of westerly granite due to increase in σ_2/σ_3 ratios. Singh et al. (1998) also observed similar strength enhancement in rock mass at site due to σ_2.

The deformation modulus also gets enhanced when rock mass is subjected to true-triaxial compression. This enhancement is 95.4%, 184.9%, 192.7%, 559.9%, 357.9% and 32.3% at joint dip $\theta = 0°$, 20°, 40°, 60° 80° and 90° respectively as given in Table 10. The maximum enhancement (559.9%) is at $\theta = 60°$ whereas at $\theta = 90°$, enhancement is minimum (32.3%). Further, it is observed that percentage maximum enhancement in modulus value is always higher than the enhancement in strengths at all joint inclination θ.

4. Expressions for deformation modulus

The results from experimental study are further used to develop expressions for predicting modulus values of rock mass under triaxial and true-triaxial compression. In triaxial compression state two different approaches namely joint factor (Ramamurthy, 1993) and Janbu (1963) were incorporated. The approaches are discussed here in detail.

Table 10. Maximum enhancement (%) in engineering parameters for rock mass

	Maximum enhancement (%)	
Dip of critical joint set θ (°)	σ_1	$E_{tj50\%}$
0	36.9	95.4
20	105.2	184.9
40	192.5	192.7
60	309.2	559.9
80	73.9	357.9
90	26.1	32.3

5. Joint factor, J_f approach

The joint factor J_f can be estimated for rock mass specimen by calculating joint frequency, J_n, joint inclination parameter, n and shear strength along joint, r as per procedure suggested by Ramamurthy (1993), Ramamurthy and Arora (1994) and Singh et al. (2002). The modulus values E_j in unconfined compression stress (UCS) and triaxial compression states are derived as below.

5.1. UNCONFINED COMPRESSION STRESS STATE

The deformation modulus in UCS ($\sigma_3 = 0$) will be found by using Equations (5) and (6) as reported by Singh et al. (2002).

$$\frac{E_j(\sigma_3 = 0)}{E_i(\sigma_3 = 0)} = \exp(bJ_f) \tag{5}$$

where

$$J_f = \frac{J_n}{n \cdot r} \tag{6}$$

and E_i is modulus of intact rock material, 'b' is a coefficient for E_j and varies with types of failure mode in rock mass as below:

Splitting : −0.020
Shearing : −0.020
Sliding : −0.060
Rotation : −0.040

5.2. TRIAXIAL STRESS STATE

Modulus value, E_j at any confining pressure, σ_3 can be estimated by using the following suggested Equation (7) which is developed using results of extensive testing on jointed block mass models under uniaxial and triaxial stress states (see Figure 10).

$$\frac{E_j(\sigma_3 = 0)}{E_j(\sigma_3)} = 1 - 0.93 \exp\left[-0.087\left(\frac{\sigma_{cj}}{\sigma_3}\right)\right] \tag{7}$$

The correlation coefficient for above equation is very good ($r^2 = 0.91$) and σ_{cj} is uniaxial compressive strength of rock mass specimen and can be calculated using following Equation (8) suggested by Singh et al. (2002).

$$\sigma_{cj} = \sigma_{ci} \exp(aJ_f) \tag{8}$$

The coefficient 'a' varies depending upon modes of failure as below:

Splitting: −0.0123
Shearing: −0.0122

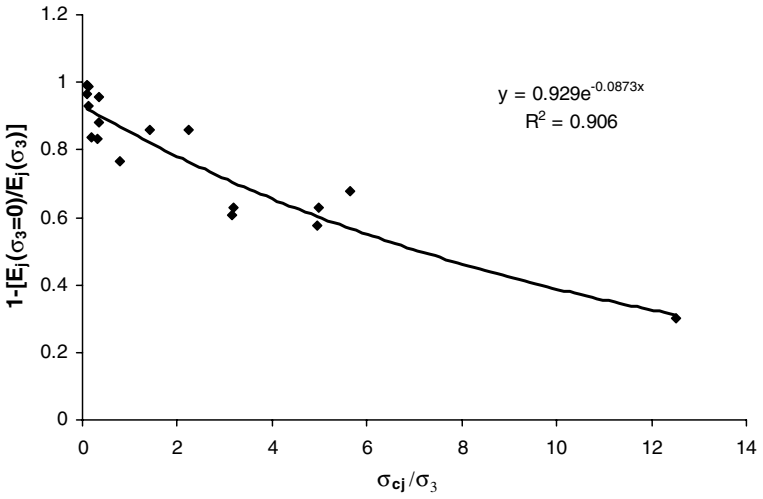

Figure 10. Estimation of E_j (σ_3) for rock mass in triaxial stress conditions.

Sliding: −0.0400
Rotation: −0.0250

5.3. PREDICTION OF MODULUS

The J_f of rock mass specimen is estimated using the method suggested by Ramamurthy (1993) and Singh et al. (2002). The J_f varies with joint configuration of rock mass. The Equations (5) and (8) were used to evaluate modulus, E_j and compressive strength, σ_{cj} in unconfined compression state respectively for different joint dip (see Table 11). Once σ_{cj} and E_{tj50} are known, the modulus, E_j (σ_3) at any confining pressure can be predicted using the Equation (7). The E_j increases with increasing σ_3 at all inclinations θ. Modulus values estimated using above equations show U shaped anisotropy with joint inclination θ as shown in Figure 11. It can be seen from Figure 11 that predicted modulus is not increasing noticeably with increase in σ_3 levels as observed in case of experimental results. The values are much higher than experimental at $\theta = 0°$ and 90° and significantly lower at rest of inclinations. The parameters n in J_f concept (Ramamurthy, 1993) is basically derived from assumption that rock material shows U-shaped anisotropy and such material behaviour is exhibited in unconfined compression state only. The increase in confining stress changes the shape of anisotropy curve and as such use of J_f poses limitations while dealing with deformation behaviour under confinement. This fact can also be confirmed by comparison of experimental and predicted values of modulus in Table 12.

Table 11. Estimation of σ_{cj} and E_j for rock mass specimen using J_f approach

Specimen ($s=0.5$, $r=0.75$)	Failure mode	Failure surface	$\beta=$ (90°−θ)	J_n/m	n	J_f	J_f (critical)	σ_{cj} (MPa)	E_j (MPa)
A0	Splitting	1	90	32.5	1.00	43.3	43.3	7.92	2046.8
		2	0	19.5	0.81	32.1			
A20	Shearing	1	70	38.5	0.63	81.5			
		2-A	6.6	6.4	0.58	14.7	186.1	1.39	117.7
		2-B	46.6	32.1	0.23	186.1			
A40	Sliding	1	50	26.5	0.31	113.9	113.9	0.14	5.2
A60	Sliding	1	30	25.5	0.05	680	680	2.1×10^{-11}	9.3×10^{-15}
A80	Rotation	1	10	12.3	0.46	35.7			
		2-A	53.4	36.2	0.36	136.3	136.3	0.44	20.9
		2-B	73.4						
A90	Shearing	1	0	6.5	0.81	43.3			
		2	90	39.2	1.00	32.1	43.3	7.03	1669.1

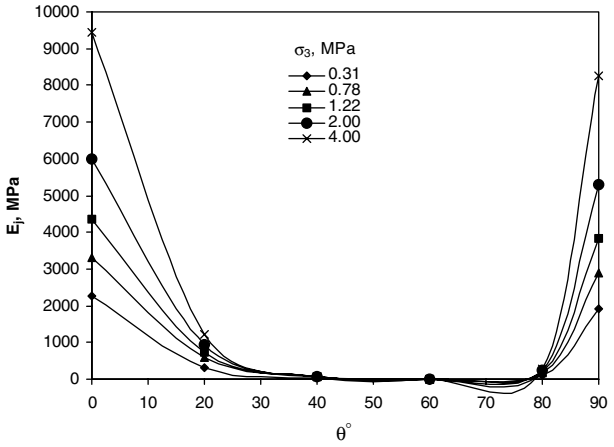

Figure 11. Prediction of modulus at different confining pressures using J_f concept.

6. Janbu's coefficients approach

The modulus values (initial and tangent modulus) of rock mass obtained at different stress levels are given in Tables 6 and 7. The triaxial tests on intact specimen show that modulus of intact rock also increases with increasing confining stresses. Janbu (1963) proposed empirical expression for estimating initial modulus of soils and intact rock at any confining stress as given by Equation (9).

$$E_i = K_i P_a \left(\frac{\sigma_3}{P_a}\right)^{n_i} \tag{9}$$

where K_i and n_i are called Janbu's coefficients and depends on rock type. The P_a is atmospheric pressure and equals to 0.101325 MPa. This equation is further used to

Table 12. Comparison of E_j values obtained from different approaches

	E_j (MPa)								
	$\sigma_3 = 0.31$ MPa			$\sigma_3 = 0.78$ MPa			$\sigma_3 = 1.22$ MPa		
θ (°)	Experimental	Janbu approach	J_f approacn	Experimental	Janbu approach	J_f approach	Experimental	Janbu approach	J_f approach
0	380.5	378.9	2276.1	711.5	595.5	3325.1	718.0	741.4	4342.2
20	200	209.2	317.8	456.4	384.6	578.2	464.1	516.6	746.1
40	84.5	78.3	49.1	142.2	174.7	61.6	298.8	257.8	65.6
60	32.9	92.5	1.3×10^{-13}	124.3	178.1	1.3×10^{-13}	189.6	244.7	1.3×10^{-13}
80	357.9	345.6	117.4	503.2	451.6	182.5	517.7	514.1	211.7
90	631.5	640.9	1916.9	671.4	702.9	2900.6	723.8	735.0	3822.3

develop empirical expression for tangent deformation modulus (E_{tj} or E_{tm50}) for jointed rock mass.

6.1. JANBU'S (1963) EQUATION FOR ROCK MASS

The Equation (9) of Janbu (1963) is modified to use for rock mass as below:

$$E_{im} = K_m P_a \left(\frac{\sigma_3}{P_a}\right)^{n_m} \tag{10}$$

where, E_{im} is initial modulus of rock mass, K_m and n_m are Janbu coefficients for rock mass, which are influenced by joint geometry and joint properties of rock mass. The extensive triaxial testing results on intact and rock mass are used to evaluate the coefficients K_i, K_m and n_i, n_m for intact and rock mass respectively. The K_i and n_i for intact rock are estimated by plotting log–log plot of E_i/P_a against σ_3/P_a. Similarly K_m and n_m at different dipping of joint set-I are also evaluated as shown in Figures 12a and b. The ratio of K_i/K_m and n_i/n_m for intact and rock mass show good

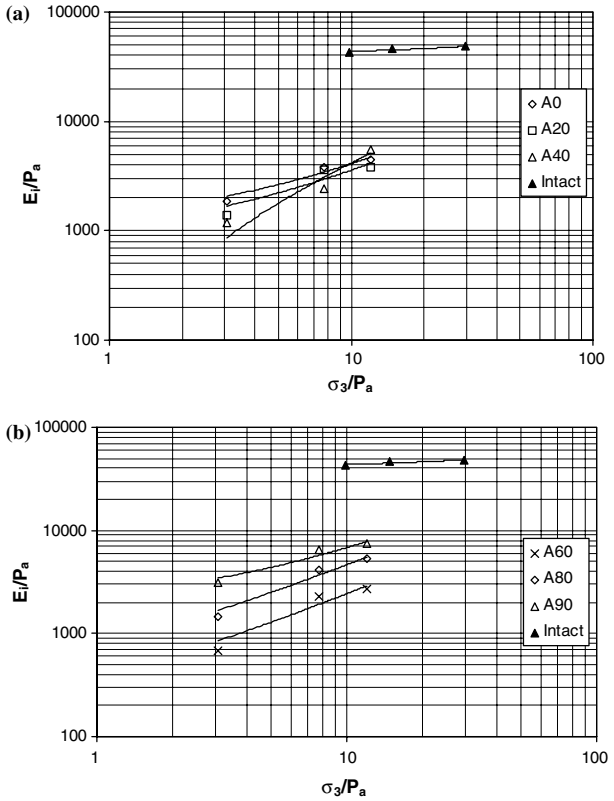

Figure 12. Log–log plot of E_i/P_a against σ_3/P_a for rock mass specimens: (a) intact, A0, A20, A40 and (b) intact, A60, A80, A90.

correlation with joint configuration as can be seen Figures 13a and b. The expressions for K_m and n_m are suggested as below:

$$\frac{K_i}{K_m} = 9.86 \exp\left[2.16 \cos\left(\frac{\pi}{3} - \theta\right)\right] \tag{11}$$

$$\frac{n_i}{n_m} = 0.29 \exp\left[-0.97 \cos\left(\frac{\pi}{3} - \theta\right)\right] \tag{12}$$

where θ is dipping of the joint set-I.

6.2. FORMULATION OF EXPRESSION

The experimental results show that the ratio of initial modulus (E_{im}) and deformation modulus (E_{tm50}) at 50% failure stress vary non-linearly with increasing confining stress for rock mass. For any rock mass, the empirical expression for deformation modulus is obtained as under

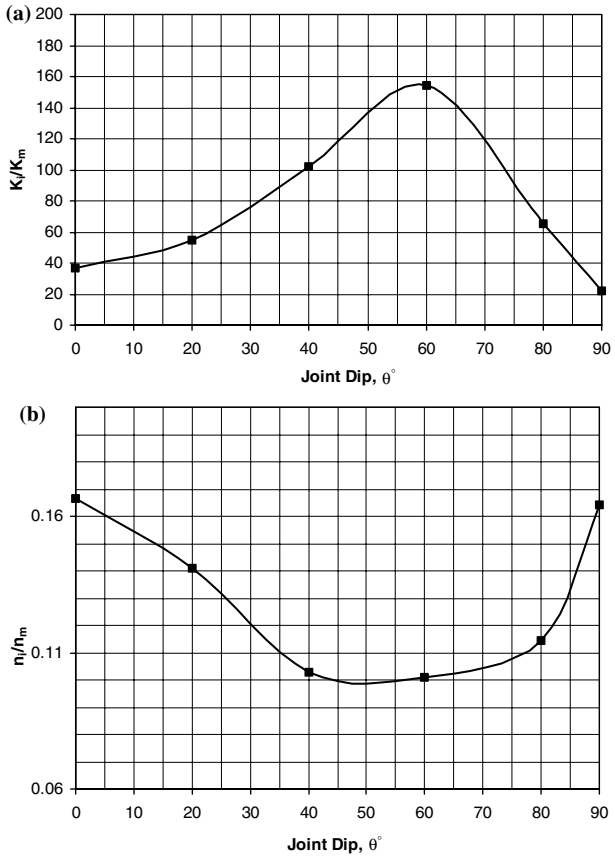

Figure 13. Variation of Janbu's coefficients: (a) K_i/K_m, (b) n_i/n_m with joint dip, θ.

$$\frac{E_{\mathrm{tm50}}}{E_{\mathrm{im}}} = \frac{P}{\left(\frac{\sigma_3}{\sigma_{\mathrm{ci}}}\right)^q} \tag{13}$$

The σ_{ci} is uniaxial compressive strength of intact model rock. The P and q are joint geometry parameters and are dependent on dipping of joint in critical joint set-I. The suitable correlations are also suggested for P and q with θ (see Equations (14) and (15)) with good correlation ($r^2 = 0.88$).

$$P = \exp[-0.019\theta] \tag{14}$$

$$q = 0.12\exp[0.018\theta] \tag{15}$$

The inclination of joint θ is measured in degree. Further, substituting the expression for E_{im} in Equation (13), one can get expression of E_{tm50} as below:

$$E_{\mathrm{tm50}} = \frac{PK_{\mathrm{m}}P_{\mathrm{a}}\left(\frac{\sigma_3}{P_{\mathrm{a}}}\right)}{\left(\frac{\sigma_3}{\sigma_{\mathrm{ci}}}\right)^q} \tag{16}$$

6.3. PREDICTION OF MODULUS

The deformation modulus of a rock mass can be predicted by using Equation (16). The input parameters and testing needed are

i. Uniaxial compressive strength test on small cylinder of intact rock to get σ_{ci}.
ii. Triaxial compression tests at three convenient σ_3 on intact rock to get Janbu's coefficients K_{i} and n_{i} for intact rock.
iii. For a joint configuration of rock mass, parameters K_{m}, n_{m}, P and q can be estimated using Equations (11), (12), (14) and (15).
iv. The rock joints are assumed smooth with average joint friction angle of 36.8° obtained in laboratory.

The deformation modulus of rock mass specimens used in the present experimental study is predicted using Equation (16) and required input parameters are calculated as above suggested guidelines. Thus modulus values are calculated at different confining pressures 0.31, 0.78. 1.22, 2.0, 2.5 and 4.0 MPa using the suggested Equation (16) and plotted in Figure 14.

As expected, the modulus values are increasing at all dipping with increasing confining stress, σ_3 (see Figure 14). Further, it is observed that modulus values are highest at $\theta = 0°$ and minimum between 40° and 60°. The anisotropy also decreases with increasing the level of σ_3.

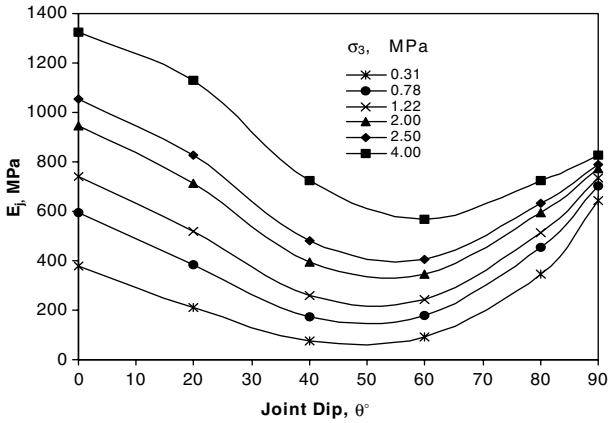

Figure 14. Prediction of modulus at different confining pressures using Janbu's coefficients approach.

7. Comparison of two approaches

The modulus values predicted using the Janbu (1963) and J_f (Ramamurthy, 1993) approaches are presented along with the experimental data for comparison as shown in Table 12. The modulus values are minimum at $\theta = 60°$ and maximum at $\theta = 90°$ obtained by both approaches and show anisotropy at all confining stresses. Table 12 explains that the proposed Janbu's (1963) coefficient approach back predicts the values much closer to experimental results than the joint factor approach. It can be seen that joint factor approach may not be applicable in describing the deformation behaviour of rock mass under confining stress state because J_f assumes U shaped anisotropy behaviour of jointed rock mass, which is possible in UCS conditions only. In the field a method should be selected based on input parameters available. It can be seen that both approaches require entirely separate type of input parameters for their applicability. Hence, the use of any approach in field solely depends upon availability of parameters at the site suiting with the requirement of that method. Further Janbu coefficient approach is recommended over joint factor approach.

8. Modulus in true-triaxial stress state

The modulus value E_j ($= E_{tj} = E_{tm50}$) value in triaxial stress state is once known using Janbu's coefficients and joint factor approaches as discussed above. Then, based on the extensive data of true-triaxial test results, the expression of E_j in true-triaxial stress states ($\sigma_2 > \sigma_3$) is suggested as in Equation (17) and also can be represented as in Figure 15.

$$\frac{E_j(\sigma_2 > \sigma_3)}{E_j(\sigma_2 = \sigma_3)} = 1 + T\left(\frac{\sigma_2}{\sigma_3 - 1}\right)^r \tag{17}$$

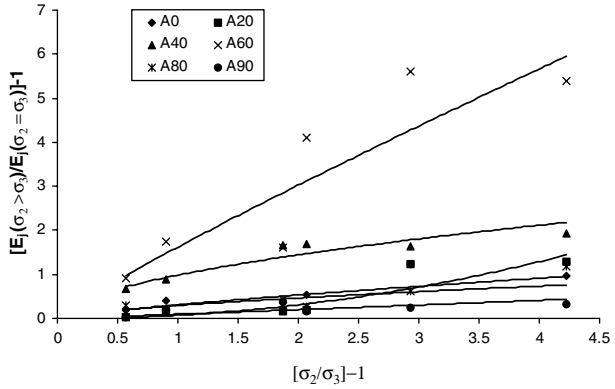

Figure 15. Estimation of E_j ($\sigma_2 > \sigma_3$) in rock mass under true-triaxial stress compression.

where T, r joint inclination parameters and vary with inclination of joint set-I as given in Table 13. Once the E_j value in triaxial stress state is known by any of the approach discussed above, the Equation (17) can be conveniently used for prediction of modulus at any joint dip θ of rock mass under true-triaxial stress conditions at any σ_2/σ_3 level.

9. Discussion and conclusions

In the present study, a large amount of results were available from model testing on rock mass with different joint geometries and stress conditions. The expressions suggested are though of empirical in nature are obtained through careful planning of experimental programme. The trend of variation of modulus values with inclination and stress state are in agreements with theoretical and fundamental thoughts of rock mass behaviour. Thus one can trusted with these equations for prediction of deformation modulus with fair accuracy though medium interlocking ($s = 0.5$) and smooth joint ($\phi_j = 36.8°$) will have to be assumed. The following are the main conclusions derived from present study.

i. The deformation modulus of rock mass is influenced due to intermediate principal stress σ_2 similar to enhancement in triaxial compressive strength. The enhancement is significant (559.9%) and is more than the enhancement in strength (309.2%).

Table 13. Parameters T and r at different inclination, θ

θ (°)	β (°)	T	r
0	90	0.31	0.78
20	70	0.07	2.06
40	50	0.98	0.55
60	30	1.62	0.9
80	10	0.29	0.67
90	0	0.1	1.05

ii. The modulus enhancement in rock mass with joint geometries corresponding to $\theta = 40°$ and 60° is more than in case of joint geometries of $\theta = 0°$, 20°, 80° and 90°. Thus weak rocks are subjected to more modulus enhancement than comparatively harder rocks.
iii. The anisotropy in modulus is seen with joint inclination θ. This anisotropy reduces with increase in σ_2/σ_3 ratio which, reflects that the joints influence the deformation characteristics of rock mass at low confining pressure only whereas the effects of joints diminishes with increase in confinement level.
iv. The joint factor (Ramamurthy, 1993) and Janbu (1963) coefficients are used to develop expressions for predicting modulus of rock mass under triaxial and true-triaxial stress states. The equations developed need input parameters; UCS and triaxial test results at three convenient confining pressures and joint geometry along with stress state to which rock mass is subjected. The joint factor approach gives very conservative results when used under confining stress conditions hence Janbu coefficient approach is recommended over joint factor.

Acknowledgements

The work presented in this paper is a part of the research study carried out by first author under the supervision of the co-author at Indian Institute of Technology Delhi for his PhD degree. The First author express his gratitude to authorities at Rewa Engineering College Rewa, Madhya Pradesh where he is working as Reader in Civil Engineering for deputing him at IIT Delhi for this study. The First author is also thankful to Government of India for providing QIP fellowship during tenure of the PhD programme.

References

Bieniawski, Z. T. (1978) Determining rock mass deformability: experience from case histories, *International Journal of Rock Mechanics and Mining Sciences & Geomechanics Abstracts*, **15**, 237–247.

Goodman, R. E. (1989) *Introduction to Rock Mechanics*, Second Edition, John Wiley and Sons.

Haimson, B. and Chang, C. (2000) A new true triaxial cell for testing mechanical properties of rock and its use to determine rock strength and deformability of westerly granite, *International Journal of Rock Mechanics and Mining Sciences*, **37**, 285–296.

Heuze, F. E. (1980) Scale effects in the determination of rock mass strength and deformability, *Rock Mechanics*, **12**, 167–192.

Huang, T. H., Chang, C. S. and Yang, Z. Y. (1995) Elastic moduli for fractured rock mass, *Rock Mechanics and Rock Engineering*, **28**(3), 135–144.

Janbu, N. (1963) Soil compressibility as determined by oedometer and triaxial test, *Proceedings of the European Conference on Soil Mechanics and Foundation Engineering, Wiesbaden*, **1**, 19–25.

Li, C. (2001) A method for graphically presenting the deformation modulus of jointed rock masses, *Rock Mechanics and Rock Engineering*, **34**(1), 67–75.

Ramamurthy, T. (1993) Strength and modulus responses of anisotropic rocks, *Comprehensive Rock Engineering*, **1**, 313–329.

Ramamurthy, T. and Arora, V. K. (1994) Strength prediction for jointed rocks in confined and unconfined states, *International Journal of Rock Mechanics and Mining Sciences & Geomechanics Abstracts*, **31**(1), 9–22.

Rao, K. S. and Tiwari, R. P. (2002) Physical simulation of jointed model materials under biaxial and true triaxial stress states, Research Report, IIT Delhi, India, 30 pp.

Singh, Bhawani, Goel, R. K., Meherotra, V. K., Garg, S. K. and Allu, M. R. (1998) Effect of intermediate principal stress on strength of anisotropic rock mass, *Tunneling and Underground Space Technology*, **13**(1), 71–79.

Singh, M., Rao, K. S. and Ramamurthy, T. (2002) Strength and deformational behaviour of a jointed rock mass, *Rock Mechanics and Rock Engineering*, **35**(1), 45–64.

Tiwari, R. P. and Rao, K. S. (2003) Physical and engineering response of artificially manufactured model material and its use for rock mass testing. *Nat. Seminar on Geomechanics and Ground Control*, 24–25 September, 2003, CMRI, Dhanbad, India, pp. 219–235.

Tiwari, R. P. and Rao, K. S. (2004) Physical modeling of a rock mass under a true-triaxial stress state, *International Journal of Rock Mechanics and Mining Sciences*, **41**(supplement 1), 396–401.